Mutation of the Calmodulin Binding Motif IQ of the L-type Ca$_v$1.2 Ca^{2+} Channel to EQ Induces Dilated Cardiomyopathy and Death*[S]

Anne Blaich[‡], Sara Pahlavan[§1], Qinghai Tian[§1], Martin Oberhofer[§1], Montatip Poomvanicha[‡], Peter Lenhardt[‡], Katrin Domes[‡], Jörg W. Wegener[‡], Sven Moosmang[‡], Sandra Ruppenthal[§], Anke Scholz[§], Peter Lipp[§1], and Franz Hofmann[‡2]

From the [‡]Forschergruppe, Institut für Pharmakologie und Toxikologie, Technische Universität München, 80802 München, Germany and the [§]Institute for Molecular Cell Biology, Research Centre for Molecular Imaging and Screening; Medical Faculty; Saarland University, 66424 Homburg/Saar, Germany

Background: Mutation of the IQ motif to EQ abolished *in vitro* CDI and CDF of the Ca$_v$1.2 channel.
Results: Cardiac-specific expression of Ca$_v$1.2^{EQ} prevents CDI and CDF, reduces I_{Ca}, and induces dilated cardiomyopathy.
Conclusion: The cardiac-specific EQ mutation leads to premature death.
Significance: Survival depends on the expression of a native Ca$_v$1.2 protein.

Cardiac excitation-contraction coupling (EC coupling) links the electrical excitation of the cell membrane to the mechanical contractile machinery of the heart. Calcium channels are major players of EC coupling and are regulated by voltage and Ca^{2+}/calmodulin (CaM). CaM binds to the IQ motif located in the C terminus of the Ca$_v$1.2 channel and induces Ca^{2+}-dependent inactivation (CDI) and facilitation (CDF). Mutation of Ile to Glu (Ile1624Glu) in the IQ motif abolished regulation of the channel by CDI and CDF. Here, we addressed the physiological consequences of such a mutation in the heart. Murine hearts expressing the Ca$_v$1.2^{I1624E} mutation were generated in adult heterozygous mice through inactivation of the floxed WT Ca$_v$1.2^{L2} allele by tamoxifen-induced cardiac-specific activation of the MerCreMer Cre recombinase. Within 10 days after the first tamoxifen injection these mice developed dilated cardiomyopathy (DCM) accompanied by apoptosis of cardiac myocytes (CM) and fibrosis. In Ca$_v$1.2^{I1624E} hearts, the activity of phospho-CaM kinase II and phospho-MAPK was increased. CMs expressed reduced levels of Ca$_v$1.2^{I1624E} channel protein and I_{Ca}. The Ca$_v$1.2^{I1624E} channel showed "CDI" kinetics. Despite a lower sarcoplasmic reticulum Ca^{2+} content, cellular contractility and global Ca^{2+} transients remained unchanged because the EC coupling gain was up-regulated by an increased neuroendocrine activity. Treatment of mice with metoprolol and captopril reduced DCM in Ca$_v$1.2^{I1624E} hearts at day 10. We conclude that mutation of the IQ motif to IE leads to dilated cardiomyopathy and death.

Cardiac excitation-contraction (EC)[3] coupling links the electrical excitation of the cell membrane to the mechanical contractile machinery of the heart (1, 2). An important step in EC coupling is the transient rise in [Ca^{2+}]$_i$ caused by an influx of Ca^{2+} through the Ca$_v$1.2 channel and the subsequent Ca^{2+} release from the sarcoplasmic reticulum (SR) through ryanodine receptor 2 (RyR2) into the "fuzzy space" (3). The [Ca^{2+}] in the fuzzy space is further controlled by the Na$^+$-Ca^{2+} exchanger (NCX) (4–6). The relative high [Ca^{2+}] in this space inactivates the Ca$_v$1.2 channel by Ca^{2+}-dependent inactivation (CDI) (1, 7) and terminates thereby Ca^{2+} entry to avoid Ca^{2+} overload and arrhythmias (7). Ca^{2+} triggers a second process called Ca^{2+}-dependent facilitation (CDF). The physiological role of CDF is not entirely clear, but it may serve to offset partly reduced Ca^{2+} channel availability at high heart rates (8, 9). Both types of regulation involve direct binding of the Ca^{2+} sensor protein calmodulin (CaM) to the Ca$_v$1.2 channel (7, 10–12) and activation of Ca^{2+}/CaM-activated protein kinase II (CaMKII) (8, 11, 13–16).

CaM binds to the IQ motif located at amino acids 1624–1635 of the Ca$_v$1.2 carboxyl terminus (10, 11, 17, 18). Isoleucine 1624 is essential for CaM binding. The mutation I1624E decreased the affinity of the IQ motif for CaM approximately 100-fold *in vitro* (11, 16). As a consequence, the I/E mutation abrogated CDF and CDI of L-type Ca^{2+} currents expressed in *Xenopus* oocytes (16).

To clarify the physiological significance of the I/E mutation, we created a mouse line that carried the I1624E mutation in the Ca$_v$1.2 gene (19). Because mice homozygous for the I/E mutation died early during embryogenesis (19), we crossed the heterozygous Ca$_v$1.2$^{+/I1624E}$ mouse to the floxed Ca$_v$1.2$^{L2/L2}$

TABLE 1
Nomenclature and genotype of mouse lines

Mouse line	Genotype[a]
WT	$Ca_v1.2^+/Ca_v1.2^{L2}$
I/E	$Ca_v1.2^{I1624E}/Ca_v1.2$- + activated MCM-Cre
Ctr	$Ca_v1.2^+/Ca_v1.2$- + activated MCM-Cre
KO	$Ca_v1.2^-/Ca_v1.2$- + activated MCM-Cre

[a] +, wild-type gene; −, Cre-inactivated $Ca_v1.2$ gene; L2, floxed wild-type gene generating a wild-type protein or after Cre excision an inactivated $Ca_v1.2$ gene; I1624E, $Ca_v1.2$ gene containing the mutated IQ motif; activated MCM-Cre, tamoxifen-activated Cre construct.

mice (20) and to mice expressing the tamoxifen-inducible Cre recombinase (MerCreMer (MCM)) under the control of the α-myosin heavy chain promoter (21). This line allows the cardio-specific induction of the Cre recombinase by tamoxifen injection in adult mice (21). Electrophysiological analysis of L-type $Ca_v1.2$ currents in cardiac myocytes (CMs) from these I/E mice revealed that the cardiac I_{Ca} was decreased and showed no regulation by CDI and CDF (19). Furthermore, the channel showed kinetic properties that suggested that the channel had permanently adopted CDI kinetics regardless of the permeating ion (19). This finding was not expected because previously the I/E mutation was associated with a loss of the Ca^{2+}-dependent acceleration of channel inactivation (11, 16).

Analysis of the mouse line carrying the heart-specific I/E mutation was hindered by the well documented finding that the MCM-Cre mouse by itself shows a transient phenotype after activation of the Cre construct by tamoxifen (22–24). To distinguish between a potentially Cre-induced phenotype and the I/E induced alteration, we used four mouse lines: the $Ca_v1.2^{I1624E} \times$ MCM (I/E) line, the $Ca_v1.2^{+/L2} \times$ MCM (Ctr) line, the $Ca_v1.2^{+/L2}$ (WT) line, and the $Ca_v1.2^{L2/-} \times$ MCM (KO) line (see also Table 1). These mouse lines allowed us to differentiate phenotypes induced only by activation of the MCM-Cre protein without affecting the expression of a wild-type $Ca_v1.2$ protein and a phenotype induced by inactivation of the cardiac $Ca_v1.2$ gene.

Analysis of these mouse lines was performed at day 10 after activation of the Cre recombinase that removing the floxed WT $Ca_v1.2$ gene because isolated CMs from the I/E mice still showed a robust I_{Ca} (19). The analysis revealed that hearts from I/E mice had an reduced overall contractile activity and developed dilated cardiomyopathy (DCM).

EXPERIMENTAL PROCEDURES

All substances used were of the highest purity available. The $Ca_v1.2$-specific antibody used in this study has been described previously (25). Amino acid numbering is according to the *O. cuniculus* $Ca_v1.2$ sequence (GenBank accession number Q01815).

Creation of I/E Mice—Generation of mice with the I1624E mutation has been described (19). The cardio-specific $Ca_v1.2$ mutation was induced by crossing the heterozygous $Ca_v1.2^{+/I1624E}$ mouse with $Ca_v1.2^{L2/L2}$ mice (20) and with mice expressing Cre under the control of the α-myosin heavy chain promoter (MCM) (21). The intercross of the three mouse lines resulted in production of $Ca_v1.2^{I1624E/L2} \times$ MCM identified as I/E, $Ca_v1.2^{L2/+} \times$ MCM (Ctr), $Ca_v1.2^{L2/+}$ (WT), and $Ca_v1.2^{L2/L2} \times$ MCM (KO) offspring at the expected Mendelian

ratio. The experiments were performed with litter-matched mice aged 8–10 weeks on a mixed C57BL6/129Sv background. The mice were injected with 2 mg of tamoxifen (Sigma) per mouse each day for 4 days. The angiotensin-converting enzyme inhibitor captopril (0.25 mg/ml) (Sigma) and the β-blocker metoprolol (0.5 mg/ml) (Sigma) were added to the drinking water 1 week before the first tamoxifen injection. Treatment was continued until day 10 after the first tamoxifen injection. All experiments were performed 10 days after the first tamoxifen injection. All animals were maintained and bred in the animal facility of the FOR923, Institut für Pharmakologie und Toxikologie, Technische Universität München, and had access to water and standard chow *ad libitum*. All procedures relating to animal care and treatment were authorized by the "Regierung von Oberbayern" and conformed to the institutional, governmental, Directive 2010/63/EU of the European Parliament guidelines and to the Care and Use of Laboratory Animals published by the US National Institutes of Health. Anesthetized mice (1.5% isoflurane) were euthanized by cervical dislocation.

Cell Preparation—Ventricular myocytes were isolated as described (AfCS Procedure Protocol PP00000125), maintained at 37 °C, and aerated with 5% CO_2. The mouse was first injected intraperitoneally with 0.5 ml of heparin diluted in phosphate-buffered saline (PBS) to 100 IU/ml followed by anesthesia with 100 mg/ml ketamine, 2% xylazine (Rompun®) 1% acepromazin (Vetranquil®) in PBS intraperitoneally.

Heart Weight—Mice were euthanized, and the hearts were isolated. The whole heart was briefly rinsed in PBS to remove blood. The hearts were blotted dry and weighed.

Histological Analyses—Hearts were collected at the indicated time points and fixed in 4% paraformalin in PBS. Tissues were embedded in paraffin using standard procedures. Serial sections were cut at a thickness of 12 μm. The slides were stained with Masson's trichrome (Sigma) according to the manufacturer's instructions. Ventricle size and septum diameter were taken from representative sections.

Assessment of Cell Death—Heart sections were used for the quantification of cell death. The TUNEL assay (Roche Applied Science) was performed according to the manufacturer's instructions.

Molecular Analyses—Protein samples for Western blotting were separated on an 8% SDS-polyacrylamide gel and transferred to a PVDF membrane. For detection the following antibodies were used: α-actinin (Sigma A7811), phospho-T286-CaMKII (Cell Signaling 3361), CaMKII (Santa Cruz Biotechnology sc-5392), phospho-ERK1-T202/T204 and phosphor-ERK2-T185/Y187-MAPK (Sigma E7028), MAPK (ERK1/2) (Cell Signaling 9102), NCX1 (Swant, π 11–13), RyR2 (Abcam), phospho-S2808-RyR2 (Abcam), and phospho-S2814-RyR2 (Badrilla).

Telemetric ECG Recordings—Radiotelemetric ECG transmitters ETA-F20 (DSI, St. Paul, MN) were implanted, and ECGs were recorded as detailed in Ref. 26.

Echocardiography—Images were obtained using a Vevo 770 Visual Sonic scanner equipped with a 30-MHz probe (Visual Sonics Inc., Toronto, ON, Canada). The procedure was as detailed in Ref. 27.
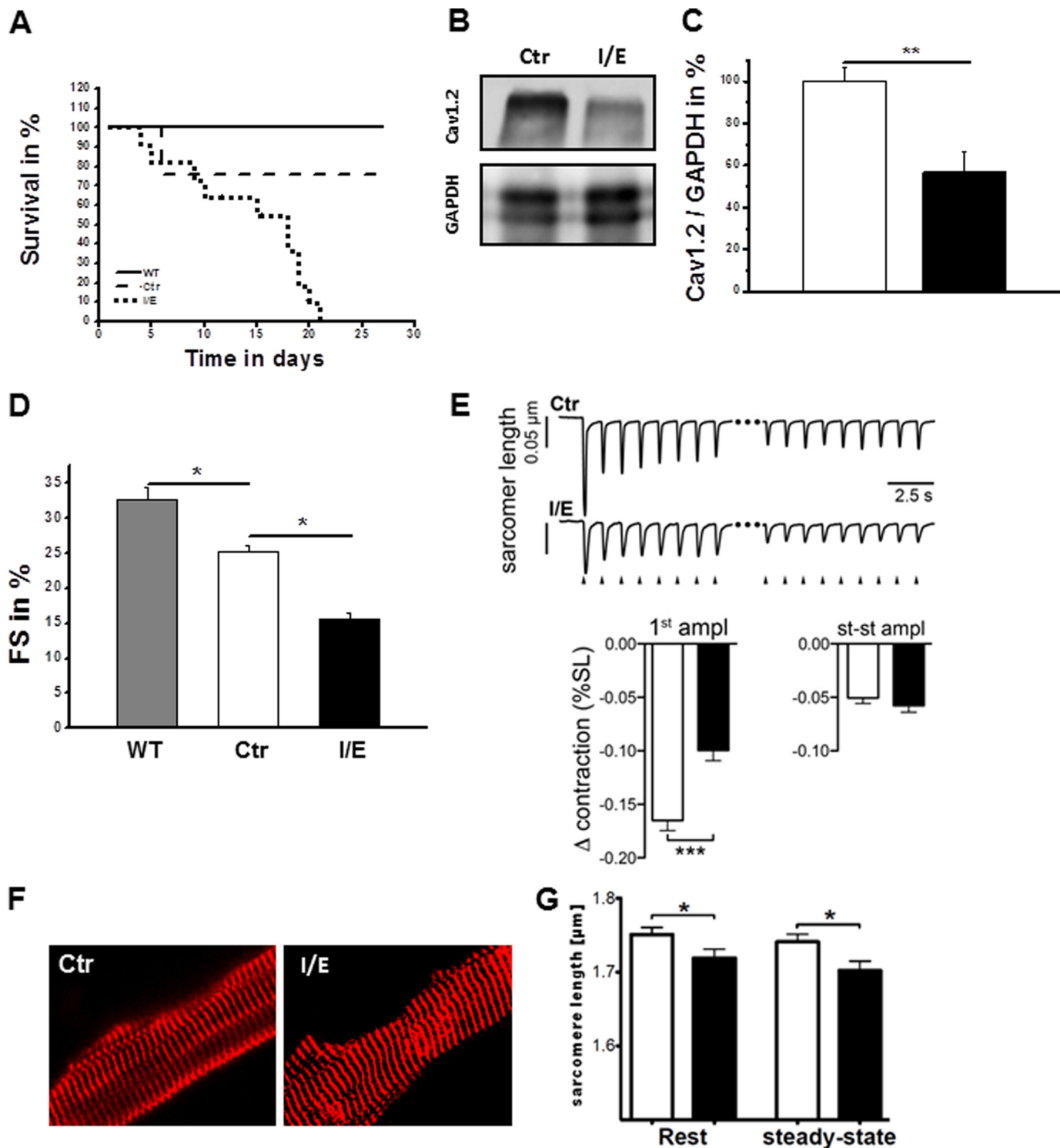
FIGURE 1. **Cardiac-specific expression of the Ca$_v$1.2$^{I/E}$ mutation leads to early mortality.** *A*, Kaplan-Meier survival curve of WT ($n = 10$), Ctr ($n = 24$), and I/E ($n = 11$) mice. At day 1, mice were injected with tamoxifen for the first time. *B*, representative Western blots for Ca$_v$1.2 and GAPDH. *C*, quantification of the Western blots in *B*. Ctr ($n = 6$) and I/E ($n = 7$) hearts are shown. *D*, echocardiographic assessment of cardiac function as FS in WT ($n = 8$), Ctr ($n = 18$), and I/E ($n = 11$) mice 10 days after the first tamoxifen injection. *E, upper*, representative examples of contraction traces. *Triangles* indicate electrical stimulation of the cells. *E, lower left*, summary of statistics for contractility determined by sarcomere length measurements after rest (first amplitude). *E, lower right*, summary of statistics for steady-state (*st*) contractility determined by sarcomere length measurements (*st-st ampl*). *F*, assessment of *Z-Z* distance by α-actinin immunocytochemistry. *G*, statistics of sarcomere length measurements in living myocytes under resting (*left*) and diastole during steady-state pacing conditions (*right*). Ctr ($n = 40/3$) and I/E ($n = 35/3$) CMs. *Gray column*, WT; *open columns*, Ctr; *black columns*, I/E. *, $p < 0.05$; **, $p < 0.01$.

Electrophysiological Recordings—Whole cell I_{Ca} or I_{Ba} was measured as described in Ref. 19, 26. All fits showed a correlation coefficient >0.98. The relation between I_{Ba} and I_{Ca} current fraction remaining 100 ms after depolarization (f_{100}) was calculated as follows: $f_{100} = (r_{100Ba}/r_{100Ca})$-1, where f_{100} is the fractional current after 100 ms, r_{100Ba} is the remain-
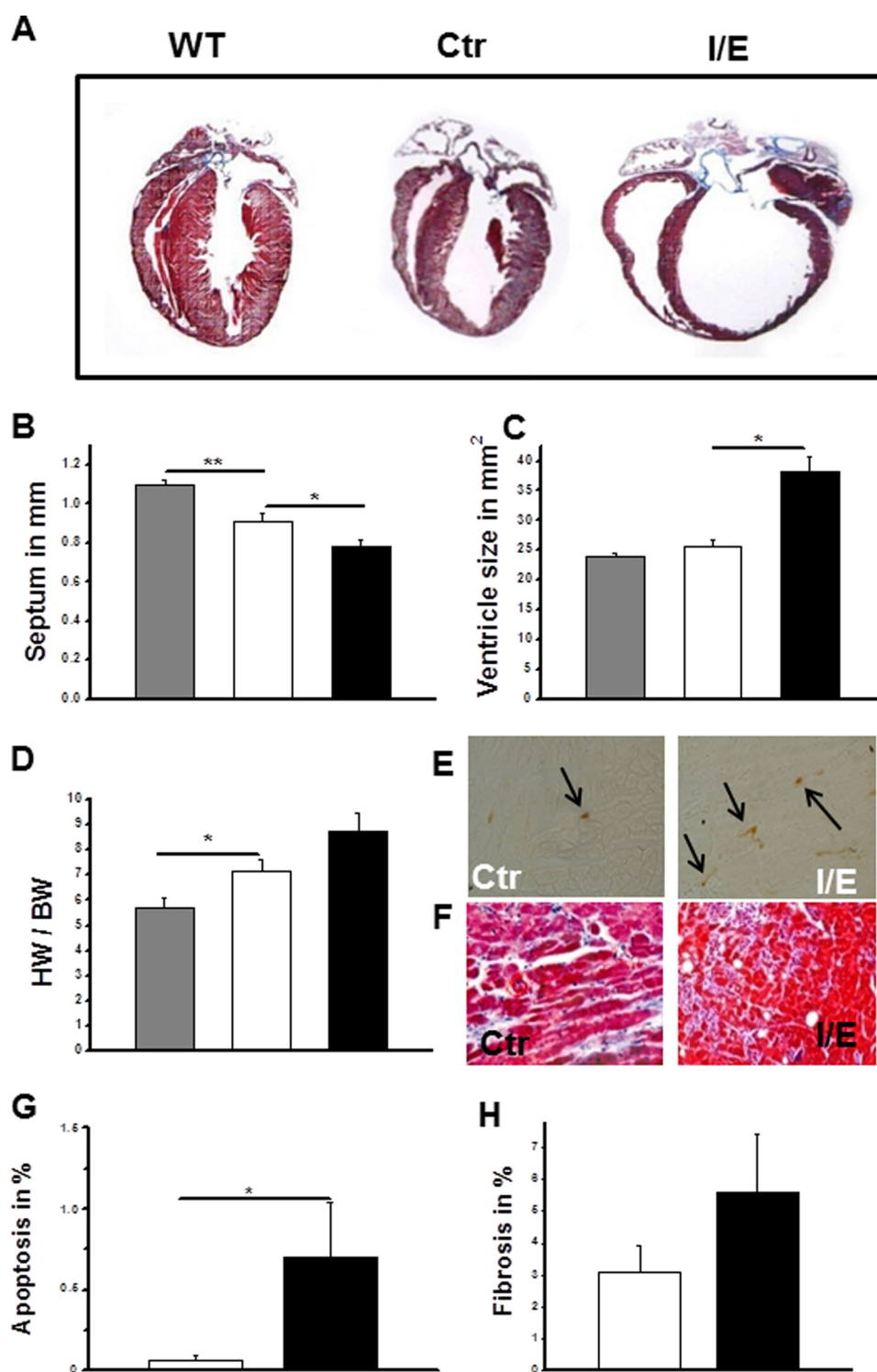
FIGURE 2. **C*tr and I/E mutation lead to remodeling of the heart at day 10.** A*, representative microscopic pictures (magnification, ×1.6) of hearts. *B*, septum diameter in mm of WT (*n* = 5), Ctr (*n* = 7), and I/E (*n* = 8) hearts. *C*, ventricle size in mm² of WT (*n* = 5), Ctr (*n* = 7), and I/E (*n* = 8) hearts. *D*, HW/BW ratio (heart weight/body weight) of WT (*n* = 7), Ctr (*n* = 8), and I/E (*n* = 13) mice. *E*, assessment of apoptosis (*brown*) with TUNEL assay. *F*, representative Masson's trichrome staining (*blue*) of myocardial tissue sections (magnification, ×200). *G*, quantitative assessment of apoptosis in Ctr (*n* = 8) and I/E (*n* = 7) hearts. *H*, quantitative assessment of fibrotic areas in Masson's trichrome-stained sections of Ctr (*n* = 13) and I/E hearts (*n* = 12). *Gray columns*, WT; *open columns*, Ctr; *black columns*, I/E. *, $p < 0.05$; **, $p < 0.01$.

ing I_{Ba} after 100 ms, and r_{100Ca} is the remaining I_{Ca} after 100 ms.

Simultaneous Calcium and Electrophysiological Recordings— Recordings were performed as described earlier (28). For

assessing the EC coupling gain we followed a protocol described in Ref. 5. Recording temperature was 22 °C.

Sarcomere Length and Calcium Measurements—For contraction and cell length measurements as well as global calcium

recordings, we used methods described previously (29). Recording temperature was 22 °C.

Statistics—Data are presented as mean ± S.E. Statistical significance was tested by using a two-tailed unpaired Student's t test or a two-way ANOVA where appropriate. The null hypothesis was rejected if $p < 0.05$. If applicable, the number of experiments are given as n = number of cells/obtained from number of animals.

RESULTS

Isoleucine 1624 of the *CACNA1C* gene has been mutated to glutamate using transgenic gene knock-in techniques (19). The resulting homozygote mice (genotype $Ca_v1.2^{I1624E}$ on both alleles) were not viable. Therefore, we cross-bred heterozygous $Ca_v1.2^{+/I1624E}$ mice with mice that expressed the floxed $Ca_v1.2$ gene (20) and the αMHC-MerCreMer construct (21) allowing tissue- and time-dependent inactivation of the $Ca_v1.2$ gene by the tamoxifen-controlled MerCreMer recombinase. The adult I/E mice had a reduced life span and died within 3 weeks after treatment with tamoxifen (Fig. 1A). ECG recordings showed that, about 1 h before death, the beat frequency decreased continuously and became arrhythmic shortly before death. Twenty percent of the control mice (Ctr) died during the first 10 days. These mice expressed a wild-type $Ca_v1.2$ gene at an unaltered expression level (supplemental Fig. 1) supporting the previous notion that the MerCreMer mice show a transient phenotype after activation of the Cre recombinase (22, 23) that is not caused by a change in the $Ca_v1.2$ channel expression (supplemental Fig. 1). In contrast to the Ctr mice, WT mice that contained a wild-type and a floxed $Ca_v1.2$ gene but no Cre recombinase were not affected by the tamoxifen injections (Fig. 1A) (for nomenclature and genotype, see Table 1).

Western blots[4] of cardiac muscle using the anti-$Ca_v1.2$ antibody (25) detected reduced protein levels in the ventricle of I/E mice compared with litter-matched control (Ctr) mice at day 10 (Fig. 1, B and C). Reduced expression of the $Ca_v1.2^{I1624E}$ protein was confirmed in the HEK293 expression system (supplemental Fig. 2). As expected from Western blotting, I_{Ca} was reduced from 2.0 ± 0.21 pA/pF (n = 18/3) in Ctr CMs to 1.1 ± 0.14 pA/pF (n = 19/3) in I/E CMs at day 10 (see Fig. 4D).

For further investigations, I/E mice were studied at day 10 after the first injection of tamoxifen.[5] Already at this stage, cardiac performance was significantly reduced as indicated by the decreased fractional shortening in the living mouse (Fig. 1D)

---

[4] We would like to add a notice of caution here. The densitometric quantification of Western blots implies accuracy that depends on the quality of the used antibodies, on the limited tissue available, and on the blots. We agree with one of our reviewers that Western blots may suggest inaccurate conclusions.

[5] Mice that contain one floxed $Ca_v1.2$ allele, one $Ca_v1.2$ I1624E allele, and the MCM-Cre construct already show at day 10 after the tamoxifen injection the electrophysiology of the mutated channel (19). This indicates to us that the WT gene product is already absent in these CMs. The Western blots always show an extensive reduced $Ca_v1.2$ band in the hearts of mice shortly before their death. This remaining $Ca_v1.2$ protein reflects the expression of the $Ca_v1.2$ gene in non-CMs, *e.g.* smooth muscle cells. The early death of the mice indicates that almost none of the floxed $Ca_v1.2$ gene escaped inactivation. This notion is supported by the finding that electrophysiological analysis of CMs at day 10 revealed no evidence for I_{Ca} mediated by an intact $Ca_v1.2$ channel protein.
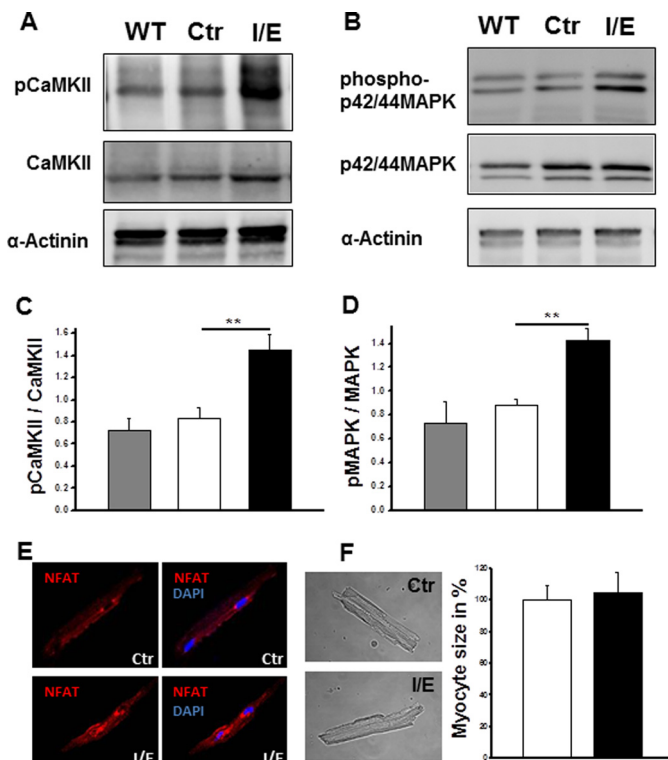

FIGURE 3. **Activation of CaMKII, MAPK, and calcineurin in Ctr and I/E mice at day 10.** *A*, representative Western blots for pCaMKII, CaMKII, and α-actinin. *B*, Representative Western blots for pMAPK (ERK1/2), MAPK (ERK1/2), and α-actinin. The shown bands represent ERK1 and 2. *C*, quantification of the Western blots in *A*. WT (n = 5), Ctr (n = 5), and I/E (n = 5) hearts are shown. *D*, quantification of the Western blots in *B*. WT (n = 5), Ctr (n = 6), and I/E (n = 5) hearts are shown. Quantification is for both bands. *E*, representative immunochemistry for NFATC3 (*red*) and nuclei (*blue*) for Ctr (n = 12/4) and I/E (n = 9/4) CMs. *F*, representative picture of CMs and quantification of size. Ctr (n = 24) and I/E (n = 13) are shown. *Gray columns*, WT; *open columns*, Ctr; *black columns*, I/E. **, $p < 0.01$.

and by the impaired myocyte contractility after rest (Fig. 1E), whereas contractility was unchanged under steady-state pacing conditions (Fig. 1E). Morphological inspection of the CMs did not reveal a severe pathology in the basic sarcomere structure as visualized by α-actinin staining (Fig. 1F). The sarcomere length of native isolated CMs was reduced in I/E mice compared with Ctr cells in both resting and steady-state diastole (Fig. 1G).

We next analyzed the cardiac phenotype *ex vivo*. Inspection of the heart showed a DCM (Fig. 2A) for I/E mice. The septum thickness of I/E hearts was decreased (Fig. 2B), whereas the ventricle size was increased (Fig. 2C) in agreement with a slightly but not significantly increased heart weight to body weight ratio (Fig. 2D). As expected for DCM (30), TUNEL staining showed an increased rate of apoptosis (Fig. 2, E and G) and changes in fibrosis (Fig. 2, F and H).

In agreement with previous studies on cardiac dilation/hypertrophy (31), the hearts with the $Ca_v1.2^{I/E}$ channel displayed increased activity levels for the CaMKII (Fig. 3, A and C) and the MAP kinase (ERK1/2) (Fig. 3, B and D) pathway. As expected, the total amount of immunologically determined ERK1/2 and RyR2 protein was not changed in the $Ca_v1.2^{I/E}$ compared with Ctr hearts. In cardiac hypertrophy (31), these pathways are often activated by the neuroendocrine axis, *i.e.* the renin-angiotensin and sympathetic systems. Interestingly, we were
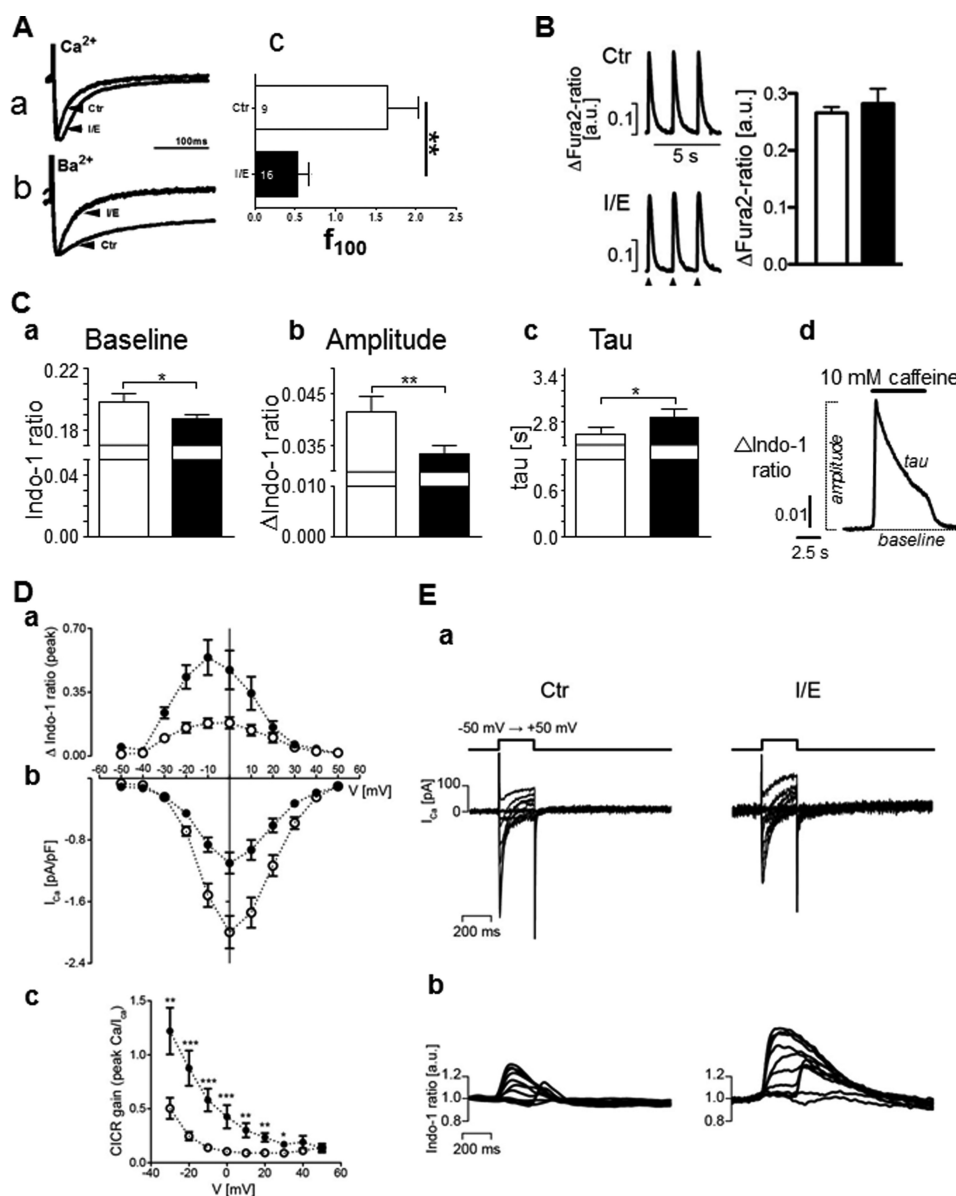
FIGURE 4. **Kinetics of I_{Ca} and Ca^{2+} release.** *A*, *a* and *b*, representative, normalized current traces of I_{Ca} (*a*) and I_{Ba} (*b*) measured in a Ctr and a I/E CM. For recording details see Ref. 19. *Ac*, f_{100} values for I_{Ba}/I_{Ca} in Ctr and I/E CMs. f_{100} is the fraction of current remaining 100 ms after depolarization calculated by the ratio of I_{Ba}/I_{Ca} present 100 ms after depolarization (11, 16). **, $p < 0.003$. *B*, steady-state Ca^{2+} transients in Fura-2-loaded Ctr and I/E CMs. *Left*, examples of Ca^{2+} transients under steady-state condition. *Right*, summary of Ca^{2+} transient amplitudes for $n = 43/3$ (Ctr) and 29/3 (I/E) CMs. Cells were stimulated at 0.5 Hz. *C*, properties of calcium handling assessed by caffeine application. Indo-1-loaded CMs were challenged by brief caffeine (10 mM) pulses. *C*, *a–c*, resting Indo-1 ratio (*a*) and amplitude of caffeine-induced Ca^{2+} transients (*b*) decreased, but time constant of Ca^{2+} decay during caffeine application increased (*c*). *Cd*, typical Indo-1 ratio trace during caffeine application. Ctr CMs, $n = 69/3$; I/E CMs, $n = 60/3$. *D*, EC gain measurements for 19/3 CMs for Ctr and I/E each. CMs were patch clamped and loaded with 100 μM Indo-1. CMs were voltage clamped at −40 mV, and a step depolarization to the indicated voltages was applied. Membrane currents (*Db* and *Ea*) and resulting Ca^{2+} transients (*Da* and *Eb*) were recorded simultaneously. *Dc*, calculated EC coupling gain. *Open symbols*, Ctr; *filled symbols*, I/E mice. *E*, representative examples for I_{Ca} and Ca^{2+} transients of a Ctr and I/E CM. *Open columns*, Ctr; *black columns*, I/E.

not able to detect an increased nuclear translocation of nuclear factor of activated T cells (NFAT) (Fig. 3E). DCM is mostly caused by a substantial loss of functional ventricle muscle as evidenced by the highly elevated apoptosis rate (32). We were therefore not surprised that the size of the CMs was not increased in $Ca_v1.2^{I/E}$ hearts (Fig. 3F).

Next, we investigated the cause of DCM in more detail. As shown previously (19), CMs expressing mutated $Ca_v1.2^{I/E}$ channels have a significantly reduced I_{Ca} loss of facilitation and no change in inactivation with Ca^{2+} as charge carrier (19). The mutation $Ca_v1.2^{I1624E}$ shortened the fast and slow inactivation

time constant for I_{Ba} to the values obtained with Ca^{2+} as charge carrier (Fig. 4A). This change in kinetics is also observed by the f_{100} value (consult "Experimental Procedures" for calculation) (Fig. 4B) (11, 16). The f_{100} value decreased significantly ($p < 0.003$) from 1.65 ± 0.38 ($n = 9$) in Ctr CMs to 0.53 ± 0.14 ($n = 16$) in I/E CMs (Fig. 4A) and indicated that, in the presence of Ba^{2+}, inactivation of the $Ca_v1.2^{I/E}$ channel was as fast as that in the presence of Ca^{2+}. These results confirm that the $Ca_v1.2^{I/E}$ channel always has the "CDI kinetics" regardless of the permeating ion. This kinetic will not lead to a reduced Ca^{2+} influx during depolarization and reduced Ca^{2+} availability in the SR.
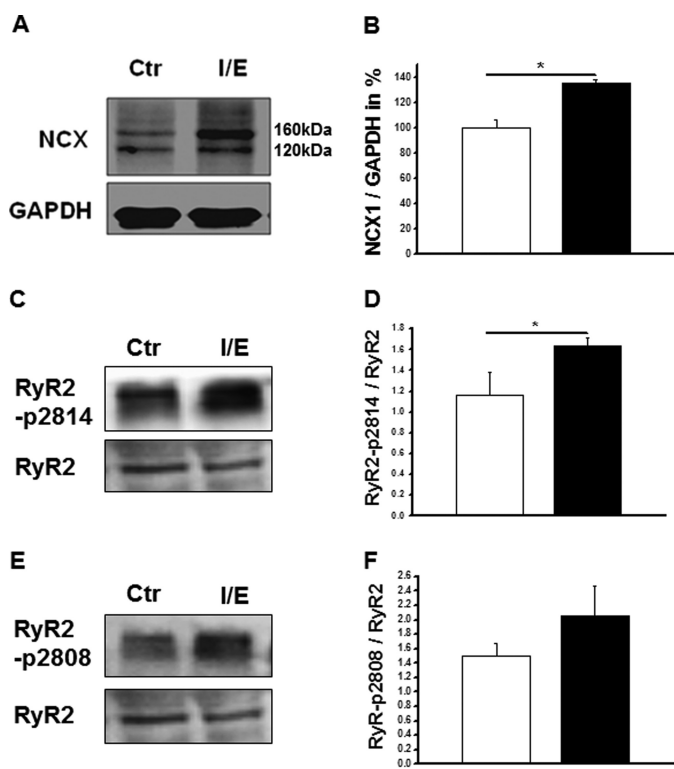
FIGURE 5. **Western analysis of NCX concentration and phosphorylation status of the RyR2.** *A*, representative Western blots for NCX1 and GAPDH. NCX1 has two bands with this antibody. *B*, quantification of the Western blots. Ctr ($n = 4$), I/E ($n = 4$). Quantification is for both bands. *C*, representative Western blots for Ser(P)^{2814} and RyR2. *D*, quantification of the Western blots. Ctr ($n = 4$), I/E ($n = 5$). *E*, representative Western blots for Ser(P)^{2808} and RyR2. *F*, quantification of the Western blots. Ctr ($n = 3$), I/E ($n = 6$). *Open columns*, Ctr; *black columns*, I/E. *, $p < 0.05$.

In agreement, shortening of isolated Ctr and $Ca_v1.2^{I/E}$ CMs (see Fig. 1*E*) and global Ca^{2+} transients (Fig. 4*B*) was unchanged, suggesting that electrical stimulation released similar amounts of Ca^{2+} from the SR under steady-state condition.

We therefore assessed the SR Ca^{2+} content by brief application of 10 mM caffeine (Fig. 4*C*). The amplitude of the caffeine-evoked Ca^{2+} transient was significantly reduced (Ctr: 0.042 ± 0.003, $n = 68/3$; I/E: 0.033 ± 0.002, $n = 67/3$). Concomitant with the decreased amplitude, the NCX-mediated Ca^{2+} extrusion extracted from the Ca^{2+} decay during caffeine application was slowed down (Ctr: 2.72 ± 0.15, $n = 57/3$; I/E: 2.88 ± 0.10, $n = 60/3$) although I/E hearts expressed slightly more NCX protein than Ctr hearts (Fig. 5, *A* and *B*). Similar results have been reported for human and rat heart failure (33–35).

Despite a decreased SR Ca^{2+} content (see Fig. 4*Cb*), steady-state contractility and global Ca^{2+} transients of the CMs were unchanged between Ctr and I/E mice. This finding strongly suggested a change in EC coupling. We therefore investigated the properties of coupling between L-type Ca^{2+} channels and RyRs by measuring EC coupling gain (Fig. 4, *D* and *E*). For this measurement, CMs were voltage clamped and repetitively depolarized (10 s at 0.5 Hz) to obtain Ca^{2+} steady-state conditions. At the end of this prepulsing period, a test depolarization from -40 mV to membrane potential between -50 mV and $+50$ mV was applied, and the resulting membrane currents as well as cytosolic Indo-1 Ca^{2+} transients were recorded simul-

taneously. As expected, the Ca^{2+} current density was reduced over the entire voltage range (Fig. 4*Db*). Under voltage clamp conditions, the Ca^{2+} transients apparently had an increased amplitude in the I/E CMs (Fig. 4*Da*). These data strongly indicated that under voltage clamp conditions the Ca^{2+} transient was higher even though the Ca^{2+} current density was decreased in the I/E mice, most likely by a combination of a decreased NCX activity (see above) and an increased RyR2 sensitivity (see below). To quantify this, we calculated the CICR gain expressed as the ratio of Ca^{2+} transient amplitude and Ca^{2+} current (Fig. 4*Dc*). This analysis strongly supported our notion that the CICR gain was significantly increased in the I/E cells.

To understand further the puzzling relationship between CM behavior (higher EC coupling gain) and functional parameters (*e.g.* decreased fractional shortening (FS)), we investigated the putative contributions of hormonal systems to the I/E phenotype. The observed DCM is partially caused by a loss of functional CMs and leads to activation of the sympathetic and renin-angiotensin system (30, 31). These hormone systems increase the activity of PKA and CaMKII. As expected (36), the phosphorylation of Ser^{2808} and Ser^{2814} of the RyR2 was enhanced in the I/E hearts (Fig. 5, *C–F*), suggesting a higher sensitivity of the calcium release mechanism of the RyR2 receptor.[4]

The data described so far are in good agreement with the hypothesis (30) that the phenotype of the I/E mice was in part induced by an increased activity of the neuroendocrine system. Therefore, we tested whether or not treatment of the mice with metoprolol (a cardiac β1-adrenoreceptor blocker) and captopril (an inhibitor of the conversion of angiotensin I to angiotensin II) improves the cardiac outcome. Treatment started 7 days before the first tamoxifen injection and reduced the dilated cardiomyopathy (Fig. 6*A*). We substantiated this macroscopic impression by analyzing key parameters that were aggravated in the I/E mice (see Figs. 1–3). Treatment with these inhibitors diminished or vastly reduced most changes induced by the I/E mutation: cardiac dilation was suppressed as shown by the reduced ventricle size and the septum thickness (Fig. 6*B*), and the CaMKII and MAPK pathways were less activated (Fig. 6*C*). Nevertheless, FS was still reduced in the I/E mice compared with their Ctr littermates (Fig. 6*E*).

An alternative possibility was that the observed properties were not due to the I/E mutation of the $Ca_v1.2$ channel, but were caused by the decreased incorporation of the $Ca_v1.2$ protein into the plasma membrane of the CMs. We therefore carefully compared the phenotype of the Ctr and I/E mice with mice containing two inactivated $Ca_v1.2$ alleles ($Ca_v1.2^{KO}$) 10 days after tamoxifen injection (supplemental Fig. 3). Survival rate, $Ca_v1.2$ protein expression, and FS did not significantly differ between $Ca_v1.2^{KO}$ and $Cav1.2^{I/E}$ mice. $Ca_v1.2^{KO}$ developed a similar DCM, septum thinning, and fibrosis (supplemental Figs. 4 and 5) but a higher apoptosis rate, CM size, and *Z-Z* distance (supplemental Figs. 4 and 5), suggesting that the reduction of the WT Cav1.2 channel had an additional negative impact on the heart. In agreement with these results, pCaMKII and pMAPK were significantly higher in $Ca_v1.2^{KO}$ than in Ctr hearts (supplemental Fig. 6, *A* and *B*). Treatment of the mouse lines with captopril and metoprolol resulted in the expected
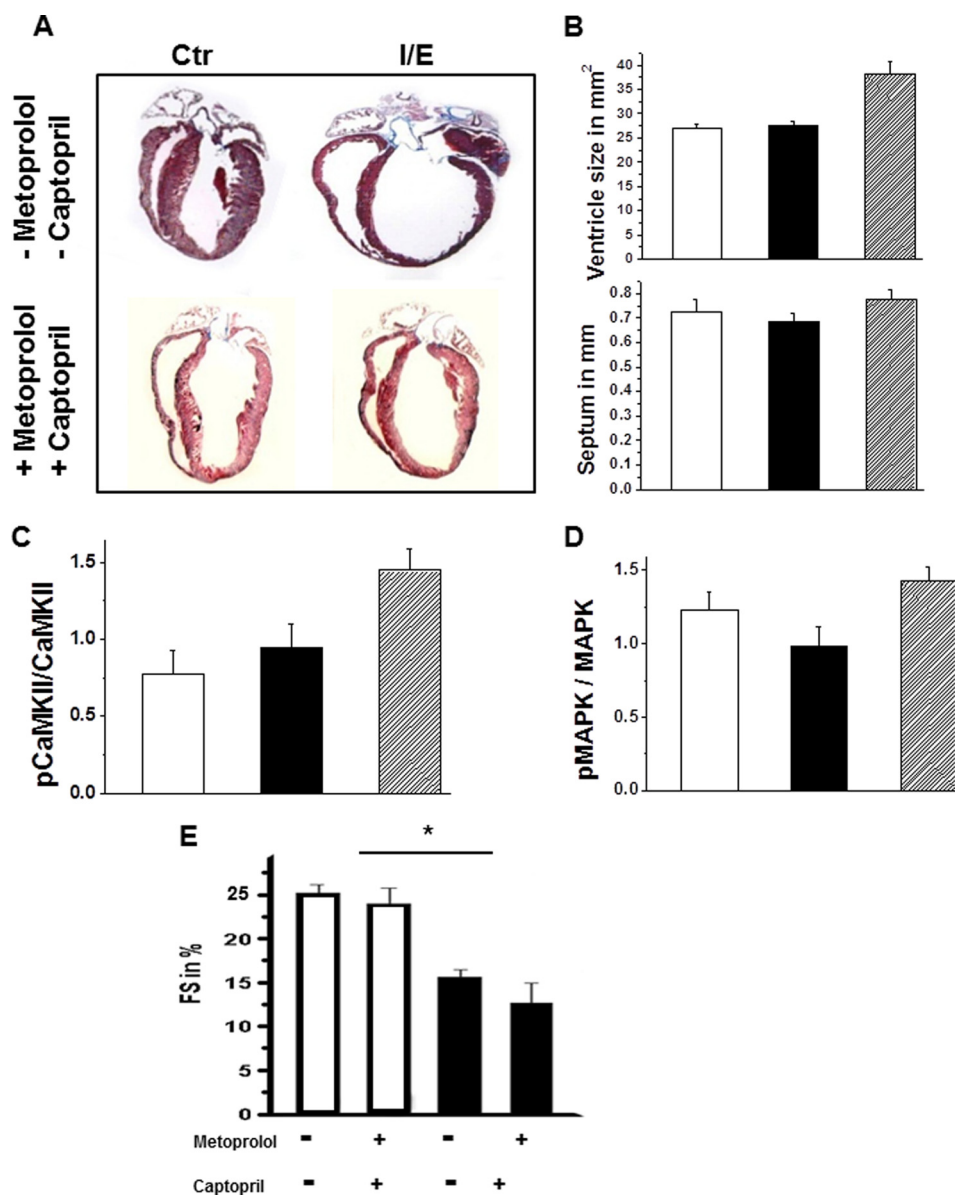
FIGURE 6. **Effects of metoprolol and captopril on Ctr and I/E mice at day 10.** *A*, representative microscopic pictures (magnification, ×1.6) of hearts at day 10 from mice that were treated with and without metoprolol and captopril. *B*, *upper*, ventricle size in mm² of Ctr ($n = 9$) and I/E ($n = 11$) from mice treated with metoprolol and captopril, and I/E ($n = 8$) from untreated mice. *B*, *lower*, septum diameter in mm of Ctr ($n = 9$) and I/E ($n = 11$) from mice treated with metoprolol and captopril, and I/E ($n = 8$) from untreated mice. *C*, quantification of the Western blots for pCaMKII and CaMKII. Ctr ($n = 4$) and I/E ($n = 7$) from mice treated with metoprolol and captopril, and I/E ($n = 5$) from untreated mice are shown. *D*, quantification of the Western blots for pMAPK and MAPK. Ctr ($n = 5$) and I/E ($n = 7$) from mice treated with metoprolol and captopril, and I/E ($n = 5$) from untreated mice. *E*, echocardiographic assessment of cardiac function as FS in Ctr −metoprolol/captopril ($n = 18$), Ctr +metoprolol/captopril ($n = 10$), I/E −metoprolol/captopril ($n = 11$), and I/E +metoprolol/captopril ($n = 10$) mice. *, $p < 0.05$ between Ctr and I/E mice. *Open columns*, Ctr; *black columns*, I/E; *hatched columns*, I/E from untreated mice.

decreased development of DCM in CTR, $Ca_v1.2^{I/E}$, and $Ca_v1.2^{KO}$ mice. However, fractional shortening was severely impaired in the $Ca_v1.2^{KO}$ mice, if treated with captopril and metoprolol (supplemental Fig. 6C). These different pharmacological sensitivities of I/E *versus* KO hearts further supported the notion that the I/E mutation not only reduced $Ca_v1.2$ expression but affected other functions by its inability to bind CaM with high affinity.

DISCUSSION

Mutation of the IQ motif to EQ in the C terminus of the $Ca_v1.2$ channel reduced the *in vitro* affinity of the channel for CaM and abrogated or abolished CDI and CDF (11, 16). We generated a mouse line in which the cardiac $Ca_v1.2$ channel carried this mutation and showed that CDI and CDF of the Cav1.2 are absent in CMs expressing the I/E mutation (19). Under voltage clamp condition, the gain of Ca^{2+} release was significantly affected by this mutation suggesting an "altered EC coupling." EC coupling depends on the amplitude, kinetics, and spatial features of the Ca^{2+} signal in the microdomain of the fuzzy space (3). The $[Ca^{2+}]$ in this space is shaped by the activity of the $Ca_v1.2$ channel, the RyR2, and the NCX exchanger. In a recent paper, Acsai *et al.* estimated that during SR Ca^{2+} release $[Ca^{2+}]$ in the fuzzy space reached $10–15$ μM within milliseconds (37). We have no direct evidence about the $[Ca^{2+}]$ concentration in the dyadic space, but the experiments of Fig. 4 suggest significant alterations of signal-

ing in this coupling space. These changes or adaptations might at least in part be brought about by the chronic activation of the sympathetic and renin-angiotensin system, leading to an increased phosphorylation of the RyR2 accompanied by a sensitization of the Ca^{2+} release mechanism (36, 38).

The phosphorylation and presumably activation of CaMKII and Erk1/2 are induced by similar factors. It has been reported that wall stress and activation of $G\alpha_q/\alpha_{11}$-coupled receptors such as the AII receptor activate CaMKII and the MAPK pathways that contribute to cardiac hypertrophy (for review, see Ref. 31). However, signaling through the MAPK pathway is complicated. Depending on the MAPK isozyme, translocation of NFAT to the nucleus may be inhibited or promoted. Further research is needed to analyze these pathways.

The I/E mutation had no significant effect on the structure of the CMs despite slight decreases in the cross-striation distance (Fig. 1*G*). This finding is strongly contrasted by the $Ca_v1.2^{KO}$ mice that developed a significantly increased CM size and increase in cross-striational distance within 10 days.

Both types of mice rapidly developed dilated cardiomyopathy. In our search for the cause of this severe phenotype, we noticed a lower resting $[Ca^{2+}]$ and a decreased loading of the SR. As observed in heart failure (6, 39), the NCX protein was increased. The global decrease in NCX activity assessed during caffeine application might be a result of structural remodeling, often observed during cardiac diseases such as T-tubular loss during remodeling (40). Such a remodeling process will lead to a lower surface/volume ratio and thus decrease the global functional Ca^{2+} removal through NCX. The $Ca_v1.2^{I/E}$ channel was expressed at a lower rate in the heart as also observed in the HEK expression system. This reduction contributed significantly to the observed phenotype.

Measurement of the contractility of isolated $CM^{I/E}$s did not show a reduction, whereas a reduced cardiac force development was present in the *in vivo* situation (see reduced FS). This discrepancy is most likely caused by the fact that the performance of the intact heart has to be considered as the combination of single myocyte contractility and the number of contributing myocytes. Analysis of the I/E hearts (see Fig. 2) revealed severe apoptosis of cardiac myocytes and an increased fibrosis. These findings strongly support the notion that a lower number of functional myocytes contribute to the overall force development and thus leading, despite a maintained contractility at the cellular level, to a decreased organ performance. To compensate the decreased cardiac function, the mouse increased the activity of the sympathetic and renin-angiotensin system to overcome the loss of functioning myocytes. Chronic hormonal stimulation leads to cellular loss through apoptosis and eventually to cardiac dilation as reported by several groups (for review, see Ref. 30). Similar results have been reported when the number of cardiac $Ca_v1.2$ channels was reduced (41).[6] A DCM phenotype was also observed after certain inflammatory, metabolic, or toxic insults which result in a significant loss of working myocardium (42).

The DCM of the I/E mice was caused by an initially reduced influx of Ca^{2+} during depolarization. This reduction was caused not only by a change in channel kinetics but also by a reduced expression of the $Ca_v1.2^{I/E}$ protein leading to decreased peak I_{Ca}. A recent publication suggested that activated CaMKII represses cardiac transcription of the $Ca_v1.2$ gene (43) and prevents CM hypertrophy (1, 31) as found in this mouse model. In humans, DCM has been associated with either a "defective force transmission" or a "defective force generation" (44). As discussed above, the DCM associated with the $Ca_v1.2^{I/E}$ mutation qualifies for the group caused by a defective force generation because the Ca^{2+} content of the SR is inadequate to provide an adequate cardiac output. Similar considerations apply to the phenotype of the total $Ca_v1.2^{KO}$ mice, suggesting that part of the phenotype observed may be attributed to a general loss of the $Ca_v1.2$ channel protein resulting in apoptosis.

Upon deletion of the wild-type allele, expression of the $Ca_v1.2^{I/E}$ gene led to a reduced Ca^{2+} influx resulting in a smaller global Ca^{2+} transient by reduced fractional Ca^{2+} release and contractility of myocytes. To compensate this, the tonus of the various neurohormonal systems increased leading to an increased EC coupling gain, transiently compensated (*i.e.* "normalized") contractility and cardiac hypertrophy (1, 31, 45). During the course of chronic increased neurohormonal stimulation, myocyte loss by apoptosis begins, and the heart enters a vicious circle of increased hormonal levels, transiently compensated contractility, and higher apoptotic loss of myocytes until compensation fails and the heart goes into DCM. Interfering with the signaling of some of these neuroendocrine factors reduced the development of DCM significantly, but could not affect apoptosis and the reduction in whole heart force development. These findings support the notion that force development and cardiac hypertrophy can be triggered by independent pathways as suggested by the work of many research groups (see 1, 22, 31, 45).

REFERENCES

1. Bers, D. M. (2008) Calcium cycling and signaling in cardiac myocytes. *Annu. Rev. Physiol.* **70,** 23–49
2. Bers, D. M. (2002) Cardiac excitation-contraction coupling. *Nature* **415,** 198–205
3. Lederer, W. J., Niggli, E., and Hadley, R. W. (1990) Sodium-calcium exchange in excitable cells: fuzzy space. *Science* **248,** 283
4. Lipp, P., Egger, M., and Niggli, E. (2002) Spatial characteristics of sarcoplasmic reticulum Ca^{2+} release events triggered by L-type Ca^{2+} current and Na^+ current in guinea pig cardiac myocytes. *J. Physiol.* **542,** 383–393
5. Altamirano, J., and Bers, D. M. (2007) Voltage dependence of cardiac excitation-contraction coupling: unitary Ca^{2+} current amplitude and open channel probability. *Circ. Res.* **101,** 590–597
6. Bers, D. M. (2002) Cardiac Na/Ca exchange function in rabbit, mouse, and man: what's the difference? *J. Mol. Cell. Cardiol.* **34,** 369–373
7. Anderson, M. E. (2001) Ca^{2+}-dependent regulation of cardiac L-type

---

[6] A major difference between this study and that of Goonasekera *et al.* (41) is that in Ref. 41, 25 mg/kg tamoxifen per day was given for 5 days (equals approximately 0.75 mg/mouse per day for a 30-g mouse), whereas in this study 2 mg/mouse per day was given for 4 days. The higher concentration given in this study does activate Cre in all CMs that express the MCM construct. According to Ref. 21, the MCM construct is expressed in >70 to >80% of all CMs.

Ca²⁺ channels: is a unifying mechanism at hand? *J. Mol. Cell. Cardiol.* **33,** 639–650

8. Maier, L. S., and Bers, D. M. (2002) Calcium, calmodulin, and calcium-calmodulin kinase II: heartbeat to heartbeat and beyond. *J. Mol. Cell. Cardiol.* **34,** 919–939

9. Ross, J., Jr., Miura, T., Kambayashi, M., Eising, G. P., and Ryu, K. H. (1995) Adrenergic control of the force-frequency relation. *Circulation* **92,** 2327–2332

10. Halling, D. B., Aracena-Parks, P., and Hamilton, S. L. (2006) Regulation of voltage-gated Ca²⁺ channels by calmodulin. *Sci. STKE* **2006,** er1

11. Zühlke, R. D., Pitt, G. S., Deisseroth, K., Tsien, R. W., and Reuter, H. (1999) Calmodulin supports both inactivation and facilitation of L-type calcium channels. *Nature* **399,** 159–162

12. Peterson, B. Z., DeMaria, C. D., Adelman, J. P., and Yue, D. T. (1999) Calmodulin is the Ca²⁺ sensor for Ca²⁺-dependent inactivation of L-type calcium channels. *Neuron* **22,** 549–558

13. Anderson, M. E., Braun, A. P., Schulman, H., and Premack, B. A. (1994) Multifunctional Ca²⁺/calmodulin-dependent protein kinase mediates Ca²⁺-induced enhancement of the L-type Ca²⁺ current in rabbit ventricular myocytes. *Circ. Res.* **75,** 854–861

14. Xu, L., Lai, D., Cheng, J., Lim, H. J., Keskanokwong, T., Backs, J., Olson, E. N., and Wang, Y. (2010) Alterations of L-type calcium current and cardiac function in CaMKIIδ knockout mice. *Circ. Res.* **107,** 398–407

15. Yuan, W., and Bers, D. M. (1994) Ca-dependent facilitation of cardiac Ca current is due to Ca-calmodulin-dependent protein kinase. *Am. J. Physiol.* **267,** H982–993

16. Zühlke, R. D., Pitt, G. S., Tsien, R. W., and Reuter, H. (2000) Ca²⁺-sensitive inactivation and facilitation of L-type Ca²⁺ channels both depend on specific amino acid residues in a consensus calmodulin-binding motif in the α₁C subunit. *J. Biol. Chem.* **275,** 21121–21129

17. Van Petegem, F., Chatelain, F. C., and Minor, D. L., Jr. (2005) Insights into voltage-gated calcium channel regulation from the structure of the Caᵥ1.2 IQ domain-Ca²⁺/calmodulin complex. *Nat. Struct. Mol. Biol.* **12,** 1108–1115

18. Kim, J., Ghosh, S., Nunziato, D. A., and Pitt, G. S. (2004) Identification of the components controlling inactivation of voltage-gated Ca²⁺ channels. *Neuron* **41,** 745–754

19. Poomvanicha, M., Wegener, J. W., Blaich, A., Fischer, S., Domes, K., Moosmang, S., and Hofmann, F. (2011) Facilitation and Ca²⁺-dependent inactivation are modified by mutation of the Caᵥ1.2 channel IQ motif. *J. Biol. Chem.* **286,** 26702–26707

20. Seisenberger, C., Specht, V., Welling, A., Platzer, J., Pfeifer, A., Kühbandner, S., Striessnig, J., Klugbauer, N., Feil, R., and Hofmann, F. (2000) Functional embryonic cardiomyocytes after disruption of the L-type α₁C (Caᵥ1.2) calcium channel gene in the mouse. *J. Biol. Chem.* **275,** 39193–39199

21. Sohal, D. S., Nghiem, M., Crackower, M. A., Witt, S. A., Kimball, T. R., Tymitz, K. M., Penninger, J. M., and Molkentin, J. D. (2001) Temporally regulated and tissue-specific gene manipulations in the adult and embryonic heart using a tamoxifen-inducible Cre protein. *Circ. Res.* **89,** 20–25

22. Hall, M. E., Smith, G., Hall, J. E., and Stec, D. E. (2011) Systolic dysfunction in cardiac-specific ligand-inducible MerCreMer transgenic mice. *Am. J. Physiol. Heart Circ. Physiol.* **301,** H253–260

23. Hougen, K., Aronsen, J. M., Stokke, M. K., Enger, U., Nygard, S., Andersson, K. B., Christensen, G., Sejersted, O. M., and Sjaastad, I. (2010) Cre-loxP DNA recombination is possible with only minimal unspecific transcriptional changes and without cardiomyopathy in Tg(αMHC-Mer-CreMer) mice. *Am. J. Physiol. Heart Circ. Physiol.* **299,** H1671–1678

24. Buerger, A., Rozhitskaya, O., Sherwood, M. C., Dorfman, A. L., Bisping, E., Abel, E. D., Pu, W. T., Izumo, S., and Jay, P. Y. (2006) Dilated cardiomyopathy resulting from high-level myocardial expression of Cre-recombinase. *J. Card. Fail.* **12,** 392–398

25. Moosmang, S., Schulla, V., Welling, A., Feil, R., Feil, S., Wegener, J. W., Hofmann, F., and Klugbauer, N. (2003) Dominant role of smooth muscle L-type calcium channel Caᵥ1.2 for blood pressure regulation. *EMBO J.* **22,** 6027–6034

26. Blaich, A., Welling, A., Fischer, S., Wegener, J. W., Köstner, K., Hofmann, F., and Moosmang, S. (2010) Facilitation of murine cardiac L-type Caᵥ1.2 channel is modulated by calmodulin kinase II-dependent phosphorylation of Ser-1512 and Ser-1570. *Proc. Natl. Acad. Sci. U.S.A.* **107,** 10285–10289

27. Lemke, T., Welling, A., Christel, C. J., Blaich, A., Bernhard, D., Lenhardt, P., Hofmann, F., and Moosmang, S. (2008) Unchanged β-adrenergic stimulation of cardiac L-type calcium channels in Caᵥ1.2 phosphorylation site S1928A mutant mice. *J. Biol. Chem.* **283,** 34738–34744

28. Reil, J. C., Hohl, M., Oberhofer, M., Kazakov, A., Kaestner, L., Mueller, P., Adam, O., Maack, C., Lipp, P., Mewis, C., Allessie, M., Laufs, U., Böhm, M., and Neuberger, H. R. (2010) Cardiac Rac1 overexpression in mice creates a substrate for atrial arrhythmias characterized by structural remodelling. *Cardiovasc. Res.* **87,** 485–493

29. Hammer, K., Ruppenthal, S., Viero, C., Scholz, A., Edelmann, L., Kaestner, L., and Lipp, P. (2010) Remodelling of Ca²⁺ handling organelles in adult rat ventricular myocytes during long term culture. *J. Mol. Cell. Cardiol.* **49,** 427–437

30. Harvey, P. A., and Leinwand, L. A. (2011) The cell biology of disease: cellular mechanisms of cardiomyopathy. *J. Cell Biol.* **194,** 355–365

31. Heineke, J., and Molkentin, J. D. (2006) Regulation of cardiac hypertrophy by intracellular signalling pathways. *Nat. Rev. Mol. Cell. Biol.* **7,** 589–600

32. Narula, J., Haider, N., Virmani, R., DiSalvo, T. G., Kolodgie, F. D., Hajjar, R. J., Schmidt, U., Semigran, M. J., Dec, G. W., and Khaw, B. A. (1996) Apoptosis in myocytes in end-stage heart failure. *N. Engl. J. Med.* **335,** 1182–1189

33. Bers, D. M., and Despa, S. (2006) Cardiac myocytes Ca²⁺ and Na⁺ regulation in normal and failing hearts. *J. Pharmacol. Sci.* **100,** 315–322

34. Hasenfuss, G., and Pieske, B. (2002) Calcium cycling in congestive heart failure. *J. Mol. Cell. Cardiol.* **34,** 951–969

35. Pieske, B., Maier, L. S., Piacentino, V., 3rd, Weisser, J., Hasenfuss, G., and Houser, S. (2002) Rate dependence of [Na⁺]ᵢ and contractility in nonfailing and failing human myocardium. *Circulation* **106,** 447–453

36. Wehrens, X. H., Lehnart, S. E., and Marks, A. R. (2005) Intracellular calcium release and cardiac disease. *Annu. Rev. Physiol.* **67,** 69–98

37. Acsai, K., Antoons, G., Livshitz, L., Rudy, Y., and Sipido, K. R. (2011) Microdomain [Ca²⁺] near ryanodine receptors as reported by L-type Ca²⁺ and Na+/Ca²⁺ exchange currents. *J. Physiol.* **589,** 2569–2583

38. Currie, S. (2009) Cardiac ryanodine receptor phosphorylation by CaM kinase II: keeping the balance right. *Front. Biosci.* **14,** 5134–5156

39. Pogwizd, S. M., Schlotthauer, K., Li, L., Yuan, W., and Bers, D. M. (2001) Arrhythmogenesis and contractile dysfunction in heart failure: roles of sodium-calcium exchange, inward rectifier potassium current, and residual β-adrenergic responsiveness. *Circ. Res.* **88,** 1159–1167

40. Brette, F., and Orchard, C. (2003) T-tubule function in mammalian cardiac myocytes. *Circ. Res.* **92,** 1182–1192

41. Goonasekera, S. A., Hammer, K., Auger-Messier, M., Bodi, I., Chen, X., Zhang, H., Reiken, S., Elrod, J. W., Correll, R. N., York, A. J., Sargent, M. A., Hofmann, F., Moosmang, S., Marks, A. R., Houser, S. R., Bers, D. M., and Molkentin, J. D. (2012) Decreased cardiac L-type Ca²⁺ channel activity induces hypertrophy and heart failure in mice. *J. Clin. Invest.* **122,** 280–290

42. Towbin, J. A., Lowe, A. M., Colan, S. D., Sleeper, L. A., Orav, E. J., Clunie, S., Messere, J., Cox, G. F., Lurie, P. R., Hsu, D., Canter, C., Wilkinson, J. D., and Lipshultz, S. E. (2006) Incidence, causes, and outcomes of dilated cardiomyopathy in children. *JAMA* **296,** 1867–1876

43. Ronkainen, J. J., Hänninen, S. L., Korhonen, T., Koivumäki, J. T., Skoumal, R., Rautio, S., Ronkainen, V. P., and Tavi, P. (2011) Ca²⁺-calmodulin-dependent protein kinase II represses cardiac transcription of the L-type calcium channel α₁C-subunit gene (Cacna1c) by DREAM translocation. *J. Physiol.* **589,** 2669–2686

44. Fatkin, D., and Graham, R. M. (2002) Molecular mechanisms of inherited cardiomyopathies. *Physiol. Rev.* **82,** 945–980

45. Hill, J. A., and Olson, E. N. (2008) Cardiac plasticity. *N. Engl. J. Med.* **358,** 1370–1380